



Ab-initio molecular deformation barriers using auxiliary-field quantum Monte Carlo with application to the inversion barrier of water

Roi Baer*

*Department of Physical Chemistry and the Lise Meitner Minerva-Center for Computational Quantum Chemistry,
the Hebrew University of Jerusalem, Jerusalem 91904, Israel*

Received 31 March 2000; in final form 10 May 2000

Abstract

The shifted-contour auxiliary field Monte Carlo method applied within a plane waves and pseudopotential framework is shown capable of computing accurate molecular deformation barriers. The inversion barrier of water is used as a test case. A method of correlated sampling is extremely useful for deriving highly accurate barriers. The inversion barrier height is determined to be 1.37 eV with a statistical error bar of ± 0.01 eV. Recent high-level ab initio results are within the error bars. Several theoretical and methodological issues are discussed. © 2000 Elsevier Science B.V. All rights reserved.

1. Introduction

The shifted contour auxiliary field Monte Carlo [1–3] implemented within a plane waves framework is a new Quantum Monte Carlo (QMC) method for high-accuracy electronic structure computations. In two papers published recently [4,5], we have shown that the method can yield chemically accurate results for molecular structure, vibrational spectroscopy and thermo-chemistry. The work described here further explores the capabilities of this approach, testing its adequacy for predicting molecular deformation barriers. We use the inversion barrier of the water molecule, recently studied in detail from first principles by Tarczay et al. [6], as a testing ground of the method.

Some QMC results for potential barriers appear in the literature. The most popular test case is the reaction barrier of the Hydrogen exchange reaction $\text{H} + \text{H}_2 \rightarrow \text{H}_2 + \text{H}$, studied by Ceperley et al. [7] and later by Diedrich et al. [8,9]. Impressive QMC reaction barrier computations for larger systems were recently published by Grossman et al. [10], who show that diffusion Monte Carlo methods [11–13] combined with pseudopotentials [14–17] lead to accurate reaction barriers, with an error of around 0.05 eV.

While, the main goal of the work described here is to test the ability of auxiliary field Monte Carlo to describe barriers, we also discuss at some length several issues in the theory and methodology of the method. We address the problem of converging the results to basis set limit. The usual methods of quantum chemistry, which employ a Gaussian basis, are inadequate because in our method the electronic

* Fax: +972-2-6513742; e-mail: roib@fh.huji.ac.il

orbitals are represented on a grid of equally spaced points (with grid spacing δx), sampling the volume of a cube of length L . Thus, the computed properties (e.g. energy) are a function of two parameters, convergence formally achieved in the limits $L \rightarrow \infty$ and $\delta x \rightarrow 0$. An additional problem is to overcome the large statistical fluctuations in the two energies being subtracted. Here, we use the method of correlated sampling which was used in a previous work [5] to compute spectroscopic constants of N_2 .

2. Theory

2.1. Stratonovich–Hubbard transformation

The goal of the Auxiliary field electronic structure method is to allow the computation of quantum mechanical expectation values of physical observables in a system of interacting electrons:

$$\hat{H} = K^T \rho + \frac{1}{2} \rho^T V \rho, \quad (1)$$

where

$$\hat{\rho}(\mathbf{r}) = \sum_{s=\uparrow\downarrow} \psi_s^\dagger(\mathbf{r}) \psi_s(\mathbf{r})$$

is the electron density operator in 2nd quantization form; $V(\mathbf{r}, \mathbf{r}') = |\mathbf{r} - \mathbf{r}'|^{-1}$ is the positive Coulomb repulsion; and K a one-body term, including kinetic energy, external potential, and other and one-body interaction terms. See Ref. [2] for further details.

The ground state energy of the electronic system can be written as a low temperature limit involving the Boltzmann operator $\exp(-\beta \hat{H})$:

$$E_{\text{gs}} = \lim_{\beta \rightarrow \infty} \frac{\langle \Phi | \hat{H} \exp(-\beta \hat{H}) | \Phi \rangle}{\langle \Phi | \exp(-\beta \hat{H}) | \Phi \rangle}. \quad (2)$$

This expression is valid for any many-electron anti-symmetric wave function Φ not strictly orthogonal to the \hat{H} ground state, Ψ_{gs} . Typically, we choose Φ as the Hartree–Fock determinant.

The problem of computing the ratio of expectation values in Eq. (2) is extremely demanding because of the two-body part of the Hamiltonian \hat{H} . The method for doing that within the auxiliary field

approach is as follows. The Fourier transform of a Gaussian is again a Gaussian:

$$\begin{aligned} \exp\left(-\frac{1}{2} x \cdot V \cdot x\right) &\propto \int_{-\infty}^{\infty} \exp\left(-\frac{1}{2} \kappa \cdot V^{-1} \cdot \kappa\right) \\ \exp(-i \kappa \cdot \kappa) d\kappa &\propto \int_{-\infty}^{\infty} \exp\left(-\frac{1}{2} \sigma \cdot V \cdot \sigma\right) \\ &\quad \times \exp(-i \sigma \cdot V \cdot \kappa) d\sigma, \quad (3) \end{aligned}$$

where V is a positive number. Generalizing this relation, replace $x \cdot V \cdot x$ by an inner product of a vector of operators: $(\rho^T V \rho) \Delta \beta$. Now V is a positive definite matrix and $\Delta \beta$ is a small positive number. The analogous relation then becomes:

$$\begin{aligned} \exp\left(-\frac{1}{2} \hat{\rho}^T V \hat{\rho} \Delta \beta\right) &\propto \int_{\text{all } \sigma \text{'s}} \exp\left(-\frac{1}{2} \sigma^T V \sigma \Delta \beta\right) \\ &\quad \times \exp(-i \sigma^T V \hat{\rho} \Delta \beta) d\sigma. \quad (4) \end{aligned}$$

Stratonovich [18] and later Hubbard [19] used these identities to transform the Boltzmann operator $\exp(-\beta \hat{H})$ of a two-body Hamiltonian (1) into a functional integral involving Boltzmann operators of one-body Hamiltonians:

$$\begin{aligned} \exp(-\hat{H} \Delta \beta) &\propto \int_{\text{all } \sigma \text{'s}} \exp\left(-\frac{1}{2} \sigma^T V \sigma \Delta \beta\right) \\ &\quad \times \exp\left(- (K + iV\sigma)^T \hat{\rho} \Delta \beta\right) d\sigma. \quad (5) \end{aligned}$$

Here $\sigma(\mathbf{r}, \tau)$ is a time-dependent density, giving rise to a time-dependent imaginary field $iV\sigma$. The one-body auxiliary field interactions perfectly mimic the effects of the two-electron interaction in the Boltzmann operator. The Stratonovich–Hubbard formalism then replaces a two-body interaction by a one-body interaction with a fictitious electron density (of any number of electrons, not necessarily an integer) and there is an integral over all possible fictitious densities.

2.2. Monte Carlo scheme

Sugiyama et al. [20] molded the Stratonovich–Hubbard formalism into a numerical scheme by us-

ing Monte-Carlo integration for estimating the functional integral. Thus, the matrix elements of the Boltzmann operator become statistical estimates based on a random Metropolis process. In our method, we do not use a Metropolis walk. Instead, we directly sample fields from a Gaussian distribution [21]. Our sampling method for N time steps, $\beta = N\Delta\beta$ (the limit $\Delta\beta \rightarrow 0$, $N \rightarrow \infty$ is implied), the functional integral is given as a weighted average:

$$\frac{\langle \Phi | \exp(-\beta \hat{H}) \hat{H} | \Phi \rangle}{\langle \Phi | \exp(-\beta \hat{H}) | \Phi \rangle} = \frac{\left\langle \left\langle \Phi \left| \hat{H} \prod_{n=1}^N \exp[-\Delta\beta(K + iV\sigma_n(\mathbf{r}))^T \hat{\rho}] \right| \Phi \right\rangle \right\rangle_{w\{\sigma\}}}{\left\langle \left\langle \Phi \left| \prod_{n=1}^N \exp[-\Delta\beta(K + iV\sigma_n(\mathbf{r}))^T \hat{\rho}] \right| \Phi \right\rangle \right\rangle_{w\{\sigma\}}}, \quad (6)$$

where, the fictitious densities sampled from a positive definite Gaussian weight:

$$W\{\sigma_n(\mathbf{r})\} = \exp\left[-\frac{1}{2} \sum_{n=1}^N \sigma_n^T V \sigma_n \Delta\beta\right]. \quad (7)$$

While highly attractive, the application of the original formalism, as well as the direct sampling Eq. (6), for electronic structure of atoms and molecules was unsuccessful and severe statistical noise dominated the computation [21,22].

In order to better understand the source of the large statistical noise, let us expand the short time Boltzmann operator expression in powers of $\Delta\beta$:

$$\begin{aligned} & \left\langle \left\langle \Phi \left| \exp[-\Delta\beta(K + iV\sigma)^T \hat{\rho}] \right| \Phi \right\rangle \right\rangle_{w\{\sigma\}} \\ &= 1 - \Delta\beta \times (K + iV\langle \sigma \rangle_w)^T \langle \Phi | \hat{\rho} | \Phi \rangle \\ & \quad + \frac{1}{2} \Delta\beta^2 \times \dots \end{aligned} \quad (8)$$

Now, since σ 's are sampled from a zero average Gaussian distribution, the term $\Delta\beta \times i\langle \sigma^T \rangle V \langle \Phi | \hat{\rho} | \Phi \rangle$ contributes 0 to the sum. Hence, this term generates pure noise in the computation. Since, $\sigma^T V \sigma \approx \Delta\beta^{-1}$, one can infer that the noise amplitude is proportional to $\Delta\beta^{1/2}$. For small $\Delta\beta$ the noise dominates all other terms in the expansion. Thus, the fluctuations of the Monte Carlo procedure are formally infinite.

2.3. The contour shift and why it works

The breakthrough solution to this problem came when Rom, Charutz and Neuhauser [1] suggested to shift the fictitious densities $\sigma(\mathbf{r}, t)$ by a time-independent amount $-i\alpha(\mathbf{r})$ into the imaginary plane, choosing the density $\alpha(\mathbf{r})$ equal to the Hartree-Fock density. Baer, Head-Gordon and Neuhauser [2] later proved that a shift by the amount of the *exact* electron density makes the Monte-Carlo integrand stationary with respect to the fictitious fields. This brings the Boltzmann matrix element to the following form:

$$\begin{aligned} & \left\langle \Phi \left| \exp\left[-\beta\left(K + \frac{1}{2}V\hat{\rho}\right)^T \hat{\rho}\right] \right| \Phi \right\rangle \\ & \alpha \left\langle \left\langle \Phi \left| \prod_{n=1}^N \exp[-i\alpha^T V \sigma_n \Delta\beta] \right. \right. \right. \\ & \quad \left. \left. \left. \times \exp\left[-\Delta\beta\left(K + iV\sigma_n(\mathbf{r})\right)^T \hat{\rho}\right] \right| \Phi \right\rangle \right\rangle_{w\{\sigma\}}. \end{aligned} \quad (9)$$

In our formalism, it is easy to see why the contour shift reduces the statistical noise and what should be the optimal choice. Expanding the right hand side of Eq. (9) in powers $\Delta\beta$, we obtain:

$$\begin{aligned} & \left\langle \left\langle \Phi \left| \exp[-i\sigma^T V \alpha \Delta\beta] \right. \right. \right. \\ & \quad \left. \left. \left. \times \exp\left[-\Delta\beta\left(K + iV(\sigma + i\alpha)\right)^T \hat{\rho}\right] \right| \Phi \right\rangle \right\rangle_{w\{\sigma\}} \\ &= 1 - \Delta\beta \times \left[(K - V\alpha)^T \rho + i\langle \sigma^T \rangle V(\rho - \alpha) \right] \\ & \quad + \frac{1}{2} \Delta\beta^2 \times \dots \end{aligned} \quad (10)$$

Now, by choosing $\alpha(\mathbf{r}) = \rho(\mathbf{r}) = \langle \Phi | \hat{\rho}(\mathbf{r}) | \Phi \rangle$, the noisy term is fully annihilated. When the single $\Delta\beta$ step we have focused on is part of a large number of steps, Φ is on the average close to the ground state of the system and thus, the optimal α should be chosen as the ground state density. A more general result and treatment can be found in Ref. [2].

2.4. Correlated sampling

The resulting Quantum Monte Carlo method is the Shifted Contour Auxiliary Field Monte Carlo. It is a method comparable to released node quantum Monte Carlo, in that it includes no 'fixed node approximations' [23,24].

One of the most attractive features of the method is that the sampling of the fictitious densities σ is according to a universal weight, unrelated to the positions of the nuclei, given in Eq. (7). Thus, the computation of energy differences, due to the motion of the nuclei can be made using correlated sampling of the same fictitious densities for different nuclear configurations. This fact was recently used for computing the force exerted on the nuclei of the N_2 molecule [5], demonstrating that the force has a finite variance.

3. Results

In this Letter, we exercise the correlated sampling technique for computing the deformation barrier for inversion of water. The theoretical method is implemented using a grid representation for the electron orbitals and the Kosloff method for time propagation [25]. More details were described earlier in Ref. [4]. All computations are done with Troulier–Martins [26] pseudopotentials for oxygen and hydrogen, generated by the FHIPP98 computer program of Fuchs and Scheffler [27]. The pseudopotentials are produced from solutions of the atomic Dirac–Kohn–Sham equation, within the local density approximation (LDA). The exchange–correlation functional used in the atomic computation is the Perdew–Wang parameterization [28] of Ceperley and Alder’s homogeneous electron gas data [29]. Within the grid (plane waves) code the pseudopotentials is applied using a Kleinman–Bylander form [30]

The two geometries of a water molecule being compared are those used by Csaszar et al. [31] as also did Tarczay et al. [6]:

$$R_{\text{OH}} = 0.95885 \text{ (0.93411) } \text{ \AA},$$

$$\angle(\text{H–O–H}) = 104.343 \text{ (180) } ^\circ.$$

3.1. The Hartree–Fock inversion barrier

We first discuss the Hartree–Fock limit. Just as with a Gaussian basis sets, it is important to converge to the basis limit. In plane waves, in principle, one has to take two limits: reduce the grid spacing δx , and increase the cubic cell length L until the results converge to the desired accuracy.

Let us first discuss the convergence with respect to the grid spacing δx . An electron confined within the screened potential experiences an uncertainty $\delta k = 2k_{\text{max}}$ in its momentum, where

$$k_{\text{max}} = \sqrt{2\mu_e \Delta V / \hbar^2}$$

and $\Delta V = V_{\text{max}} - V_{\text{min}}$ is the difference between the smallest and largest eigenvalues of the screened potential. By Heisenberg’s principle, the minimal uncertainty in the position is then: $\delta x_c = (2\pi/\delta k)$. Thus, δx_c is the essential grid spacing, for correctly representing electronic orbitals. In Fig. 1, the convergence of the water inversion barrier height with the ratio $\delta x_c/\delta x$ is studied. It is seen that the barrier height is *not* converged when $\delta x_c/\delta x > 1$. In fact, only when $\delta x_c/\delta x > 2$ does rapid exponential convergence set in. This is because the screened potential itself depends on the density matrix. The density matrix is more sensitive to grid spacing than the orbitals, because it is determined by the multiplication of two orbitals. Thus, the density matrix is exponentially converging only after $\delta x_c/\delta x > 2$.

While the energy and other observables usually converge rapidly with grid spacing δx (once $\delta x_c/\delta x > 2$), this is not the situation with the cubic box length L . Here, an extrapolation procedure is needed. The situation is clearly depicted in Fig. 2, where the $L = \infty$ limit is determined from a polynomial fit to the computed values. Having 6 data

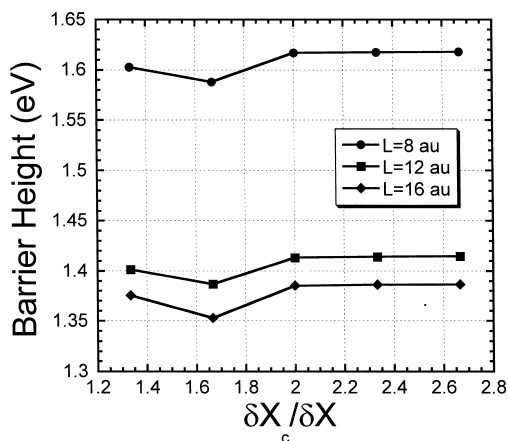


Fig. 1. Hartree–Fock inversion barrier heights vs. the grid spacing quality ratio, for several cell sizes. When the ratio is above 1 the orbitals are well represented, but the density is not. When the ratio exceeds 2.0 rapid convergence of the barrier height is achieved.

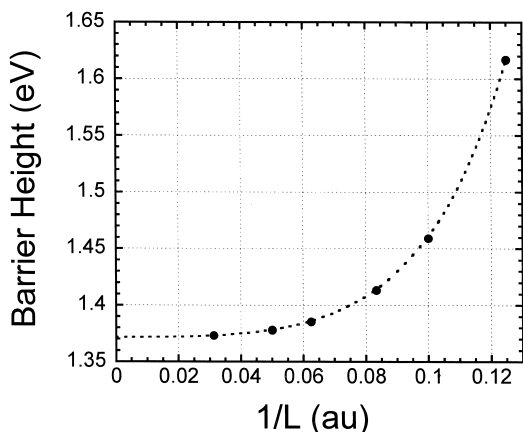


Fig. 2. Hartree–Fock inversion barrier height as a function of cubic cell length L . The calculations are with $\delta x = 0.33$ au ($\delta x_c / \delta x \approx 2$). The dotted line is a polynomial fit to the dot values (discussed in text).

points, we have made a least squares fit to the functional form $B(L) = B^{\text{HF}} + (a/L^3) + (b/L^5)$ where this form is chosen because of dipole–dipole and quadrupole interactions are present. Trying to use any form with even powers of $1/L$ resulted in a grossly unreasonable non-monotonic extrapolation curve. The form $B(L) = B^{\text{HF}} + (a/L) + (b/L^3)$ gave almost identical B^{HF} values. The converged Hartree–Fock limit of the barrier height within the pseudopotential approximation, is thus:

$$B^{\text{HF}} = 1.372 \pm 0.002 \text{ eV} \quad (11)$$

The error bar here reflects a sensitivity of the barrier height to the extrapolation procedure. This value should be compared to the all-electron Hartree–Fock limit of Tarczay et al. [6] which is 1.394 eV. We attribute the difference between the two values to the use of a DFT based pseudopotential, which partitions differently the barrier energy into SCF and correlation parts, in particular.

3.2. Inversion barrier correlation energy

Next, the contribution of correlation energy to the barrier height is determined. Here a grid spacing value of $\delta x = 0.4$ au was used and we tested two cell sizes, $L = 8$ au and $L = 12$ au. The results are shown in Fig. 3. The computations use a time step of

$\Delta\beta = 0.1$ au. To test the convergence with respect to this parameter, we also ran some computations with a time step of $\Delta\beta = 0.05$ au. The results for $L = 8$ au are also shown in Fig. 3, where it can be seen that any significant difference, if it exists, is not larger than the relevant statistical errors.

To estimate the large β limit, we exploit the asymptotically exponential form of the barrier as a function of the inverse temperature. For QMC computed barriers B_n for which $n > N_0$, where N_0 is such that $\beta_n \geq 0.5$ au, parameters B^0 , B^∞ , β_0 are found, such that the function

$$B(\beta) = B^0 \exp - \beta/\beta_0 + B^\infty (1 - \exp - \beta/\beta_0) \quad (12)$$

minimizes the RMS error,

$$\sigma_{\text{fit}} = \sqrt{\frac{1}{N - N_0} \sum_{n=N_0}^{N-1} [B(\beta_n) - B_n]^2}.$$

The parameter B^∞ is then considered the least squares estimate of the fully correlated barrier with an error, of statistical origins, $\text{S.E.} = 2\sigma_{\text{fit}}$. The estimated parameters are shown in Table 1. An important quantity is the barrier correlation energy, which is defined

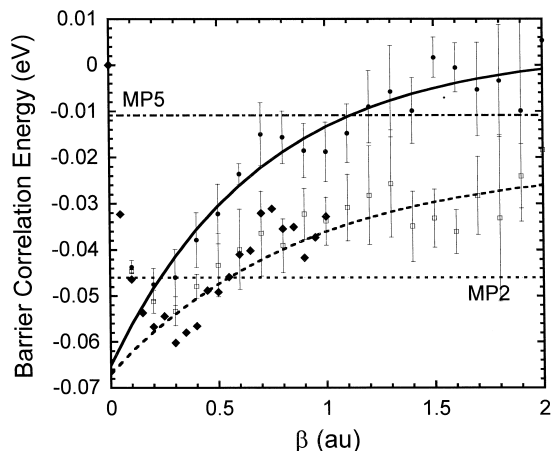


Fig. 3. Barrier correlation energy vs. inverse temperature. QMC results of $L = 8$ and 12 au (respectively, open squares, 170 K iterations; solid circles, 100 K iterations) with $\Delta\beta = 0.1$ au. Best fit functions and MP2/MP5 energy of Ref. [6] are also plotted. Diamonds in the figure are QMC results for $L = 8$ au and $\Delta\beta = 0.05$ au.

Table 1
The parameters of the fit of the QMC barrier heights to Eq. (12)

L (au)	B^0	B^∞	β_0 (au)	σ_{fit}	B^{HF}	B^{corr}
8	1.52	1.57	0.90	0.009	1.59	-0.021
12	1.32	1.39	0.71	0.004	1.39	0.003

The HF barrier B^{HF} and the barrier correlation energy, B^{corr} , are also shown. Units are eV, except where noted.

as the difference between the fully correlated barrier and the Hartree–Fock barrier:

$$B^{\text{corr}} = B^\infty - B^{\text{HF}} \quad (13)$$

is shown in Table 1.

In Fig. 3, we see that at small β values there is a significant lowering of the barrier due to some electron correlation. However, at higher β values the correlation energy is seen to have only a minute contribution. The calculations of Tarczay et al. [6] show a similar behavior when taking higher orders of perturbation theory into account: using a 2nd-order Møller–Plesset (MP) perturbation theory, a relatively large negative correlation energy is obtained, which is subsequently diminished when higher MP orders are further taken into account (see Fig. 3).

Our final value of the barrier correlation energy is $0.00 \text{ eV} \pm 0.01$. This is somewhat higher than the corresponding value of -0.011 eV calculated by Tarczay et al. [6] using coupled cluster and high-order Møller–Plesset methods, extrapolated to the full basis set limit. As noted above, the discrepancy is not surprising because of the DFT based pseudopotential.

4. Summary

The shifted contour auxiliary field Monte Carlo method, applied within a plane waves pseudopotential framework is shown able of yielding reasonably accurate deformation barriers via the correlated sampling technique. The method was applied to computing the barrier to linearity of water, and we find a correlation energy of $0.00 \pm 0.01 \text{ eV}$ and this, added to our HF barrier yields the final estimate of the barrier energy:

$$E_b = 1.37 \pm 0.01 \text{ eV} \quad (14)$$

with the error bar representing statistical errors. Non Born–Oppenheimer corrections were estimated by Tarczay et al. [6] and found smaller than the statistical error. We should note that relativistic effects and some core correlation are actually already built into the pseudopotential. Our value for the barrier energy compares favorably with the recently published, empirically based estimations of the water barrier to linearity by Polyanski et al. [32] (1.36 eV) and Kain et al. [33] (1.38 eV) and the ab initio estimations of Tarczay et al. [6] (1.38 eV).

Possible source of discrepancy between the estimates may be attributed to a pseudopotential intransferability. This is in fact the only source of uncontrolled approximation made in this computation. Here we found that an LDA based norm conserving pseudopotential leads to good results for the water barrier. In a recently submitted work on the nitrogen bond, a similar conclusion was drawn [5]. However, more experience, and perhaps careful comparisons between different pseudopotentials, needs to be gained before any definite conclusion can be made on the adequacy of norm conserving pseudopotentials for this type of high-accuracy molecular computations. Because of limited computational resources, we did not compute the correlation energy in a cell larger than $L = 12 \text{ au}$ or with a grid-spacing smaller than $\delta x = 0.4 \text{ au}$, thus correlation energy may still be slightly larger than what we have found.

The computations presented here were all performed on the CUBIOT¹ Pentium cluster, which runs the MOSIX for Linux cluster optimization software [34]. The CPU time on this system for reaching the 0.01 eV error bars was about 2 weeks. More modest error bars, around 0.04 eV take about a day of CPU time for the large cell size and several hours for the small cell size.

This work takes an additional step establishing the reliability and accuracy of the auxiliary field Monte Carlo method. The application of the method to larger systems is an important future project, since theoretical arguments as well as practical experience indicate that Quantum Monte Carlo methods scale

¹ CUBIOT cluster consists of 84 Pentium III (500 MHz) processors, each with 128 MB memory, connected by fast Ethernet (100 Mbps).

with system size somewhat better than deterministic high-correlation methods [35].

Acknowledgements

This work was supported by Israel Science Foundation founded by the Israel Academy of Sciences and Humanities. I gratefully thank D. Neuhauser, S. Shaik, R. Kosloff and A. Ben Shaul for their help and encouragement.

References

- [1] N. Rom, D.M. Charutz, D. Neuhauser, Chem. Phys. Lett. 270 (1997) 382.
- [2] R. Baer, M. Head-Gordon, D. Neuhauser, J. Chem. Phys. 109 (1998) 6219.
- [3] N. Rom, E. Fattal, A.K. Gupta, E.A. Carter, D. Neuhauser, J. Chem. Phys. 109 (1998) 8241.
- [4] R. Baer, D. Neuhauser, J. Chem. Phys. 112 (2000) 1679.
- [5] R. Baer, J. Chem. Phys., 2000, in press.
- [6] G. Tarczay, A.G. Csaszar, W. Klopper, V. Szalay, W.D. Allen, H.F. Schaefer III, J. Chem. Phys. 110 (1999) 11971.
- [7] D.M. Ceperley, B.J. Alder, J. Chem. Phys. 81 (1984) 5833.
- [8] D.L. Diedrich, J.B. Anderson, Science 258 (1992) 786.
- [9] D.L. Diedrich, J.B. Anderson, J. Chem. Phys. 100 (1994) 8089.
- [10] J.C. Grossman, L. Mitas, Phys. Rev. Lett. 79 (1997) 4353.
- [11] J.B. Anderson, Int. Rev. Phys. Chem. 14 (1995) 85.
- [12] B.L. Hammond, W.A. Lester Jr., P.J. Reynolds, Monte Carlo Methods in Ab Initio Quantum Chemistry, World Scientific, Singapore, 1994.
- [13] C.J. Umrigar, M.P. Nightingale, K.J. Runge, J. Chem. Phys. 99 (1993) 2865.
- [14] W.J. Stevens, H. Basch, M. Krauss, J. Chem. Phys. 81 (1984) 6026.
- [15] M.M. Hurley, P.A. Christiansen, J. Chem. Phys. 86 (1987) 1069.
- [16] B.L. Hammond, P.J. Reynolds, W.A. Lester Jr., J. Chem. Phys. 87 (1987) 1130.
- [17] C.W. Greeff, W.A. Lester Jr., J. Chem. Phys. 109 (1998) 1607.
- [18] R.D. Stratonovich, Dokl. Akad. Nauk SSSR 115 (1957) 1907, [translation Sov. Phys. Dokl. 2 (1958) 416].
- [19] J. Hubbard, Phys. Rev. Lett. 3 (1959) 77.
- [20] G. Sugiyama, S.E. Koonin, Ann. Phys. (N.Y.) 168 (1986) 1.
- [21] D.M. Charutz, D. Neuhauser, J. Chem. Phys. 102 (1995) 4495.
- [22] P.L. Silvestrelli, S. Baroni, R. Car, Phys. Rev. Lett. 71 (1993) 1148.
- [23] J.B. Anderson, J. Chem. Phys. 63 (1975) 1499.
- [24] S. Zhang, J. Carlson, J.E. Gubernatis, Phys. Rev. Lett. 74 (1995) 3652.
- [25] R. Kosloff, H. Tal-Ezer, Chem. Phys. Lett. 127 (1986) 223.
- [26] N. Troullier, J.L. Martins, Phys. Rev. B 43 (1991) 1993.
- [27] M. Fuchs, M. Scheffler, Comput. Phys. Commun. 119 (1999) 67.
- [28] J.P. Perdew, Y. Wang, Phys. Rev. B 45 (1992) 13244.
- [29] D.M. Ceperley, B.J. Alder, Phys. Rev. Lett. 45 (1980) 566.
- [30] L. Kleinman, D.M. Bylander, Phys. Rev. Lett. 48 (1982) 1425.
- [31] A.G. Császár, W.D. Allen, H.F. Schaefer III, J. Chem. Phys. 108 (1998) 9751.
- [32] O.L. Polyansky, P. Jensen, J. Tennyson, J. Chem. Phys. 105 (1996) 6490.
- [33] J.S. Kain, O.L. Polyansky, J. Tennyson, Chem. Phys. Lett. 317 (2000) 365.
- [34] A. Barak, O. La'adan, A. Shiloh, Scalable Cluster Computing with MOSIX for LINUX, Proc. 5th annual Linux Expo, Raleigh, May, 1999, p. 95.
- [35] Y. Shlyakhter, S. Sokolova, A. Luchow, J.B. Anderson, J. Chem. Phys. 110 (1999) 10725.